Environ. Sci. Technol. 1982, 16, 815–820

Development and Evaluation of Sunlight Actinometers

David Dulin and Theodore Mill*

Physical Organic Chemistry Department, SRI International, Menlo Park, California 94025

■ We have developed and used two binary chemical actinometers for sunlight measurements from 300 to 370 nm that have the great advantage of possessing adjustable quantum yields to provide half-lives ranging from a few minutes to several weeks in sunlight. One actinometer is the known *p*-nitroanisole (PNA)/pyridine (pyr) system in water, the half-life of which in sunlight can be varied from a few minutes to 12 h by changing the concentration of the pyridine. The other actinometer is *p*-nitroacetophenone (PNAP)/pyr, which has a half-life in sunlight ranging from several hours to 2 months and also can be adjusted by varying the concentration of pyr. Both systems are well behaved kinetically and have quantum yields invariant with wavelength from 313 to 366 nm. Neither PNA nor PNAP is volatile from water or readily sorbed, and each is easily analyzed by UV or HPLC. For PNA/pyr, ϕ = 0.44[pyr] + 0.000 28 and for PNAP/pyr, ϕ = 0.0169[pyr].

Introduction

The Toxic Substances Control Act of 1976 (PL 94-469) requires that the U.S. Environmental Protection Agency (EPA) evaluate all new chemicals for their possible adverse effects on the environment before manufacture and use are permitted. The act also provides that the manufacturers of new chemicals provide the EPA with laboratory and other test data on the fate and effects of specific chemicals that may constitute a possible hazard to a biological population. To be useful to the EPA, test data must be developed under conditions that allow meaningful interpretation in the context of environmental transport and transformation processes.

Laboratory test methods or protocols have now been developed for a variety of kinetic and equilibrium fate processes believed to be important in aquatic, atmospheric, and soil systems (*1*, *2*); other protocols are still being developed.

The photolysis protocols are designed to provide approximate or accurate rate constants for photolysis over a range of sunlight conditions commonly found in aquatic systems. However, application of the kinetic data derived from photolysis under one set of sunlight conditions to a wide range of sunlight conditions requires the use of one or more standard actinometers to monitor and integrate the variable solar irradiance during the photolysis period, which may last from a few minutes to several weeks (*1*). This study was conducted to explore, develop, and evaluate actinometers suitable for use in the sunlight photolysis protocols.

Background

General Considerations. Estimation of the rate constant for photolysis in sunlight (k_{pE}) of a specific chemical in dilute aqueous solution requires information about the absorption spectrum of the chemical, the quantum yield of the process (ϕ, the efficiency), and the intensity of sunlight as a function of wavelength, latitude, season, and, perhaps, time of day (*1*, *3*). Laboratory measurements give estimates of ϕ at selected wavelengths, and solar irradiance data are available for all regular variations in the sun's zenith and declination. Thus, in principle, k_{pE} can be estimated from laboratory measurements. However, laboratory measurements for ϕ are time-consuming, require special equipment, and can be complicated by a variety of factors; estimates of k_{pE} made in this way sometimes are subject to significant errors, although in many cases the estimates agree closely with measurements made in direct sunlight (*4*, *5*).

Estimates of k_{pE} and ϕ can also be made by direct exposure of solutions of a chemical to sunlight providing the solar irradiance is monitored in some way to account for all of the variations induced by weather, diurnal cycling, and seasonal changes (for long exposures). One way to do this is to simultaneously expose another chemical (actinometer) that has a known value of ϕ that is invariant with wavelength. Ideally, the chemical and actinometer should have similar absorption spectra and should be exposed for the same time period to ensure accurate integration of the solar irradiance available to the chemical. At the time this work began, no actinometers were available for use in sunlight for periods of days or weeks; laboratory actinometers such as *o*-nitrobenzaldehyde (*5*) typically have high values of ϕ (>0.5) and have half-lives in sunlight of a few minutes.

Kinetics of Environmental Photolysis. The upper atmosphere cuts off solar irradiance at about 290 nm (Figure 1); therefore, chemicals in the terrestrial environment can absorb photons only at this or longer wavelengths. In general the specific photochemical process that occurs cannot be predicted, although some useful generalizations have been made (*6*, *7*).

Kinetic relations governing light absorption and reaction in dilute solutions of chemicals in water have been discussed previously by Mabey et al. (*1*) and Zepp (*8*).

In sunlight, the rate constant for photolysis (k_{pE}) is given by

$$d[C]/dt = 2.3r\phi\sum L_\lambda\epsilon_\lambda[C] = k_{pE}[C] \quad (1)$$

where ϵ_λ and L_λ are the extinction coefficient and solar irradiance, respectively, at wavelength λ, ϕ is the quantum yield, which is assumed to be wavelength independent, and r is a reaction parameter characteristic of the system. Integration of eq 1 gives

$$\ln [C_0]/[C_t] = k_{pE}t \quad (2)$$

where $[C_0]$ and $[C_t]$ refer to concentrations at time zero and t.

Equation 2 may be used to estimate k_{pE} by using laboratory measurements of ϕ and ϵ_λ and tables of L_λ values to give values of k_{pE} for clear weather conditions. Equation 2 also can be used to estimate k_{pE} if losses of the chemical (C) and actinometer (A) are followed while both are exposed to sunlight; simple regression of ln (A_0/A_t) vs. ln (C_0/C_t) gives the slope S, from which the average or an environmental quantum yield for photolysis of the chemical (ϕ_{cE}) can be estimated from the outdoor experiment by using the relation

$$\phi_{cE} = \phi_a\left[\frac{1}{S}\frac{\sum L_\lambda\epsilon_\lambda{}^a}{\sum L_\lambda\epsilon_\lambda{}^c}\right] \quad (3)$$

where superscripts a and c refer to actinometer and chemical, respectively. Once ϕ_{cE} is known, eq 2 can be used

0013-936X/82/0916-0815$01.25/0

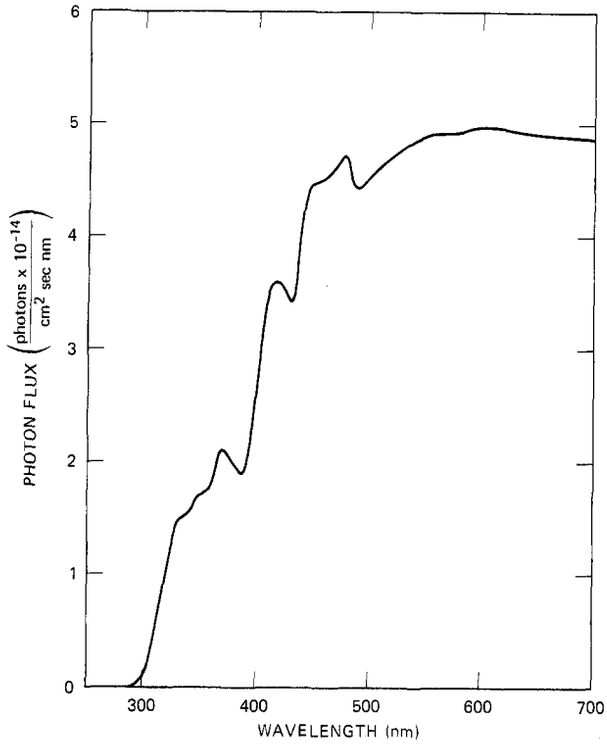

Figure 1. Solar irradiance as a function of wavelength.

to estimate k_{pE} at other latitudes and seasons in clear weather.

Equation 3 assumes that the ratio of the light absorbed by the chemical and the actinometer are constant over changes in seasons, latitudes, and sky conditions. This assumption is quite good if $\lambda \geq 350$ nm but is increasingly in error as λ approaches 300 nm because the difference between intensities of sunlight near 300 and ≥350 nm increases in winter and under cloud cover.

Another problem that arises from using eq 3 is the need to interpolate values of L_λ that are usually listed for a single date in each season (*1*, *8*) to the values of L_λ on the date of the experiment (and perhaps under cloud cover). Simple linear interpolation between seasonal values probably is accurate enough for this purpose. We estimate that L_λ will have a maximum error of 15% from the true value.

Finally, we must emphasize that ϕ_{cE} estimated in this way is a quantum yield averaged over all wavelengths; regardless of whether the value is in good agreement with a measurement of ϕ_c in a narrow wavelength interval, it does represent a "real" value applicable to exposure to the sun. In some cases, the value of ϕ estimated in this way is more useful than the value measured in the laboratory, either because ϕ is not constant with wavelength or because of special optical problems that can occur on photolysis in the laboratory but not in sunlight.

Properties of Sunlight Actinometers. For measuring sunlight intensity, chemical actinometry offers several advantages over instrumental methods, the most important being that the proper actinometer can integrate solar flux during the time and weather conditions experienced by the test chemical. Moreover the actinometer can conform to the same geometry as that of the test chemical.

Listed below are several criterions for chemical and spectral properties that we believe should be given high priority in selecting actinometers for use in sunlight. An ideal sunlight actinometer should (a) absorb light moderately and uniformly in the near UV but be relatively stable in room light, (b) have a quantum yield that is temperature and wavelength independent, (c) have a quantum yield that is independent of the concentration of the actinometer, (d) have an adjustable half-life between 0.1 and 30 days, (e) have photolysis products that do not interfere with photolysis, either chemically or spectrally, (f) be readily analyzed by conventional methods, (g) be very stable in water in the dark, (h) be moderately soluble and nonvolatile in water.

The adjustable half-life or quantum yield is perhaps the most unusual but most useful feature for a sunlight actinometer. In practice the half-life or quantum yield would be varied by changing the composition of the actinometer solution in some way to bracket the half-life of the test chemical and ensure that both actinometer and chemical were exposed to the same levels of sunlight.

The most promising approach to developing an actinometer with an adjustable half-life lies in finding suitable bimolecular photoreactions that are therefore amenable to changes in ϕ with changes in the concentration of one (usually photoinert) reactant. Photonucleophilic substitutions constitute one important class of these reactions (*9*, *10*).

In general, among substituted benzenes and naphthalenes, NO_2 substitution activates loss of OR (*10*); see eq 4, where N = N_3^-, $MeNH_2$, HO^-, R_1R_2NH, C_6H_5N; OR =

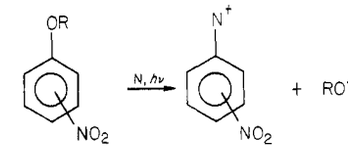

(4)

OMe, OSO_3^-. Many of these reactions follow the relation

$$\phi = k_p[N] \quad (5)$$

Experimental Procedures

Chemicals. All chemicals came from commercial sources and were used without further purifications because analyses by HPLC revealed only trace impurities in the samples.

Preparation of Reaction Solutions. All glassware used was routinely baked overnight at 580 °C. Solutions of chemicals were prepared in pure water obtained from a Milli-Q water purification system. The filter-sterilized water obtained typically shows greater than 18 mho cm resistivity and less than 1 $\mu g\ mL^{-1}$ total organic carbon, which is the detectable limit.

Reaction solutions were usually prepared from a stock solution of the chemical in acetonitrile. An aliquot of this solution was diluted with an amount of water to give a 1% or 0.1% acetonitrile in water solution. Preparation of the stock solution and subsequent dilutions were made to obtain the desired concentrations.

Laboratory Photolyses. Reaction mixtures of the chemical (4 mL) were placed either in 12-mm o.d. borosilicate (Pyrex 7740) or 11.9-mm o.d. quartz tubes and photolyzed on a merry-go-round reactor (MGRR) (Ace Glass). The irradiance source was a Hanovia 450-W medium-pressure Hg lamp contained in a borosilicate immersion well. The distance between the irradiance source and tubes was about 10 cm. The reaction temperature was the ambient operating temperature of the system (~26 °C).

The photolyses were carried out by using several different filter systems, which were placed between the Hg lamp and the reaction mixtures. In all laboratory photolyses, the borosilicate glass immersion well (8-mm total glass path length) served as a filter to screen out all light below 290 nm. The 313 and 366 nm filter systems are

Table I. Photolysis of PNA/pyr at 313 nm and 26 °C[a,b] in Pyrex

time, min	10^6[PNA], M
0	7.90
30	4.98
50	3.50
75	2.38
120	1.24
150	0.77

[a] $k_p = 1.54 \times 10^{-2}$ min^{-1}; $t_{1/2} = 44.9$ min. [b] [pyr] = 0.0124 M; $\phi(313) = 5.7 \times 10^{-3}$.

described by Calvert and Pitts (*6*). Sample tubes were removed from the MGRR at appropriate times and analyzed at the end of each experiment. We calculated ϕ from the photolysis rate constant k_p as described previously (*1*, *6*, *8*).

Actinometry with *o*-Nitrobenzaldehyde. The photochemical system was calibrated at 313 and at 366 nm by using the *o*-nitrobenzaldehyde actinometer system (*6*). In these calibration experiments, a solution of approximately 1×10^{-2} M *o*-nitrobenzaldehyde in acetonitrile was photolyzed in borosilicate or quartz tubes for reaction times as long as 16 min at either wavelength in the MGRR. The solutions were analyzed for starting aldehyde by using reverse-phase HPLC with 50% acetonitrile in water as eluent. The light incident on the tubes was then calculated according to the method of Calvert and Pitts (*6*) by using a quantum yield for *o*-nitrobenzaldehyde photolysis of 0.505. We calculated that at 313 nm I_0 varies from 2.5×10^{-6} to 3.5×10^{-6} einstein s^{-1} L^{-1} and at 366 nm varied from 6.73×10^{-6} to 8.18×10^{-6} einstein s^{-1} L^{-1}.

Sunlight Photolyses. Outdoor photolyses were carried out with pure water solutions of each chemical. Photolyzed solutions were placed in a location free of excessive reflections from walls and windows and without morning and afternoon shadows. We used 12-mm o.d. borosilicate or 11.9-mm o.d. quartz tubes held in a rack at a 45° angle to the horizon for PNA and PNAP samples and at 60° to the horizon for all other samples. The tubes were made from the same glass stock used in the laboratory photolyses. Rate constants were evaluated in the same way as laboratory photolyses rate constants.

Analyses. Most analyses were performed by HPLC on a Waters Associates chromatograph (Model 6000A pump, MV6K injector, and a M440 absorbance detector). Separations were made with a 30 cm × 4 mm μBondapak C_{18} column (reverse phase). The solvent eluent composition, UV detector wavelength, and internal standard (the internal standard in all cases *p*-nitrotoluene), if any, are given in the following table. Peak areas in the HPLC traces were determined on a Spectro-Physics Autolab Minigrator.

	mobile phase	flow rate, mL/min	detector, wavelength, nm
p-nitroanisole	50/50 CH_3CN/H_2O	2	300
p-nitroacetophenone	50/50 CH_3CN/H_2O	2	288
dibenzothiophene	75/25 CH_3CN/H_2O	2	244

Data Treatment. First-order rate constants were estimated from the regression ln (C_0/C_t) vs. time by using standard linear regression programs available in many small calculators, including the HP-97 Stat Pac. The special case of $C_t = C_0$ was not used to avoid forcing the origin through zero. The slope of the regression is k_p.

Results

***p*-Nitroanisole/Pyridine Actinometer.** One potentially useful reaction involves pyridine (pyr) substitution on *p*-nitroanisole (PNA) first described by Letsinger et al. (*11*) (eq 6). When the reactants are irradiated in water

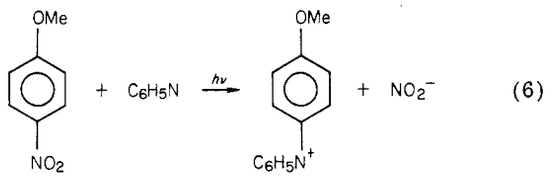

(6)

with light ≥300 nm, the reaction proceeds cleanly over 10 half-lives to give the single product. Oxygen does not affect the reaction, nor are secondary reactions of either NO_2^- or *p*-pyridinium anisole reported. The reaction slows slightly with increasing temperature, indicating a small negative activation energy (−3 kcal/mol).

The UV spectrum of PNA shows a maximum at 314 nm (log ϵ = 4.04); pyr absorbs much more weakly, with a maximum at 250 nm (log ϵ = 3.48). Consequently, even high concentrations of pyr do not absorb significant fractions of sunlight.

Our experiments used concentrations ratios of PNA:pyr of 1:10 to 1:1000 to maintain a large excess of pyr over PNA throughout the reaction and to ensure a reasonable approximation to pseudo-first-order kinetics. However, water was found to compete with pyr at the lowest pyr concentration used. Table I summarizes some typical experimental data for PNA with 0.0124 M pyr. The reaction was well behaved over two half-lives, with a half-life of 45 min. For this reaction, the quantum yield was calculated to be 5.7×10^{-3}.

The effect of varying concentrations of pyr on the value of ϕ at 313 and 366 nm is summarized in Table II. The most important features of the data are (1) the constant value of ϕ at 313 and 366 nm at three concentrations of pyr, (2) the linear relation between k_p or ϕ over a 20-fold change in pyr concentration, and (3) the competitive photoreaction of PNA with water. The range of reactivity observed here is equivalent to 15 min to 4 h for PNA/pyr exposed to bright summer sunlight. The data in Table III correlate with the relationship

$$\phi_{obsd} = 0.44[\mathrm{PYR}] + 0.000\,28 \qquad (7)$$

We performed several experiments to measure the rate constant for photolysis of PNA in sunlight (k_{pE}) using PNA solutions in quartz tubes mounted at 60° from the horizon. These values and corresponding half-lives are listed in Table III. PNA/pyr or PNA in water alone is a fast actinometer with half-lives ranging from 12 h under overcast conditions with little or no pyr to as little as 13 min in clear weather with 0.01 M pyr.

Table IV lists values of the half-life of PNA for all four seasons over a range of [pyr], calculated by using eq 1. ϕ values were measured at 313 and 366 nm and combined with the sum of $L_\lambda \epsilon_\lambda$ for absorption of PNA from 299–430 nm. L_λ values were taken from Mabey et al. (*1*). These data are plotted in Figure 2 for convenient reference in selecting a value of [pyr] to give a desired half-life of PNA.

The reader should note that all values of $t_{1/2(E)}$ in Table IV have been divided by 2.2 to convert them from values applicable to a flat water body (for which L_λ applies) to cylindrical tubes exposed to scattered light on all sides. We have compared the rates of photolysis of aqueous solutions of PNA/pyr, PNAP/pyr, and Rose bengal in open

Table II. Rate of Photolysis of PNA/pyr as a Function of pyr Concentration at 366[a] and 313 nm at 27 °C

10^5[PNA], M	[pyr], M	$10k_p$, h^{-1} [a]	$t_{1/2}$, h	$10^4\phi_{PNA}$[a,b] (366)	$10^4\phi_{PNA}$[b,c] (313)
1.0	0	0.47 ± 0.004	15	2.9	
1.0	1.0×10^{-4}	0.42 ± 0.009	17	2.7	2.4
0.79	1.24×10^{-3}	1.20 ± 0.022	5.0	9.0	
0.79	3.31×10^{-3}	2.44 ± 0.039	2.84	17	15
0.79	1.24×10^{-2}	9.24 ± 0.120	0.750	57	57

[a] At 366 nm. [b] ϕ_{PNA} values are ±12%.

Table III. Photolysis of PNA/pyr in Sunlight[a]

10^4-[pyr], M	sky, date[b]	10^2k_{pE}, min^{-1}	$t_{1/2(E)}$, h (min)
0	PC, 8:30-4:00 A29	0.22 ± 0.046	5.2
0	Cl, 11:00-4:00 J23	0.47 ± 0.012	2.4
1.00[c]	OC, 9:20-4:30 A23	0.093 ± 0.011	12.4
1.00[c]	Cl, 9:20-4:30 A25	0.27 ± 0.01	4.3
12.4	PC, 10:00-1:00 J4	0.90 ± 0.01	1.3
124	Cl, 2:00-3:00 M22	5.11 ± 0.17	0.22 (13)
124	PC, 10:18-11:00 J3	4.34 ± 0.04	0.26 (16)
124	OC, 10:40-11:00 J12	1.63 ± 0.04	0.70 (42)
124	Cl, 1:40-2:00 J12	2.63 ± 0.066	0.44 (26)
124	PC, 3:00-3:15 J12	3.30 ± 0.083	0.35 (21)

[a] [PNA] = 0.79×10^{-5} M in 10-cm quartz tubes unless otherwise noted. [b] Sky: Cl = clear, OC = overcast, PC = partly cloudy. Date: daylight hours, April (A), May (M), or June (J), date. [c] [PNA] = 1.00×10^{-5} M.

Table IV. Calculated Half-Life of PNA in Tubes as a Function of [pyr] in Sunlight at lat 40 °C[a]

	$t_{1/2}$, h			
10^4[pyr], M	spring	summer	fall	winter
0	12.0	5.9	11.6	24.7
1.00	10.4	5.2	10.1	21.5
2.00	9.2	4.6	8.9	19.0
4.00	7.5	3.7	7.2	15.4
8.00	5.4	2.7	5.3	11.2
16.00	3.5	1.7	3.4	7.2
32.00	2.1	1.0	2.0	4.2
64.00	1.1	0.56	1.1	2.3
128.00	0.56	0.29	0.55	1.2

[a] $t_{1/2} = \ln 2/2.2\phi_T \Sigma \epsilon_\lambda L_\lambda$ where $\phi_T = \phi_{pyr} + 0.000\,28$.

dishes with those in quartz tubes (at 60° from the horizon) and find a fairly consistent factor of 2.2–3, depending on the action spectrum of the solution, for the ratio of rates in dish to tube.

***p*-Nitroacetophenone (PNAP)/pyr Actinometer.** PNA/pyr is a variable quantum yield actinometer useful for short-term sunlight experiments of under 12 hours. We screened several aromatic ketones as possible long term actinometers and found that p-nitroacetophenone (PNAP) is very stable to photolysis in water with a half-life of over 5 months. Photonucleophilic substitution by pyridine on PNAP is facile, and this combination forms the basis for a second variable quantum yield actinometer with a much larger range of half-lives than PNA/pyr. The spectrum of PNAP exhibits a maximum at 275 nm (log ϵ = 4.17), with a tail extending into the solar region.

Table V summarizes the results of several experiments we performed to measure quantum yield dependence on wavelength, temperature, and [pyr] for photolysis of the PNAP/pyr system. The results show that ϕ is the same at 313 and 366 nm and the change in ϕ with [pyr] is linear over a 20-fold change in [pyr]. The relation between [pyr] and ϕ is given by the equation (r = 0.999)

$$\phi = 0.0169[\text{pyr}] \quad (8)$$

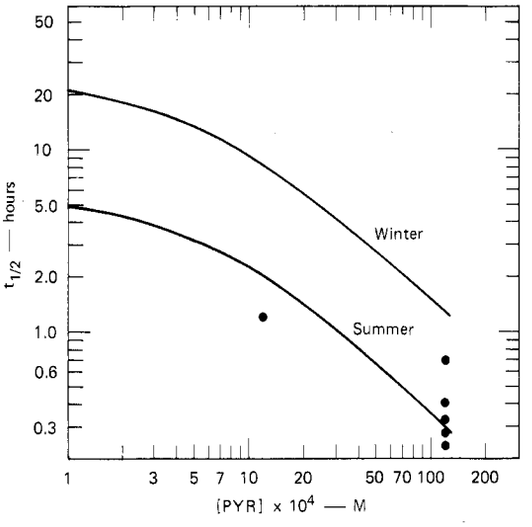

Figure 2. Calculated half-life on PNA in sunlight as a function of [pyr] at lat 40°; (●) experimental results. Values are for tube measurements.

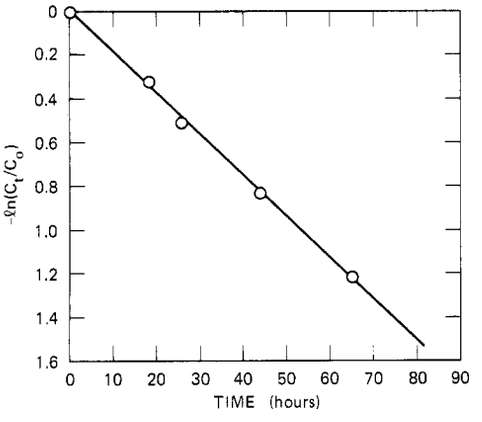

Figure 3. Photolysis of PNAP with 2.48×10^{-2} M pyr at 313 nm.

Table V. Photolysis of PNAP/pyr in Water at 313 and 366 nm and 25 and 43 °C[a]

$10^3[\text{pyr}]_0$, M	10^3k_p, h^{-1}	10^5-ϕ(313 nm)	10^5-ϕ(366 nm)
1.25	0.77 ± 0.036	3.6[b]	
4.29	1.71 ± 0.037	8.0[b]	
9.06	3.21 ± 0.19	15[b]	
12.4	9.17 ± 0.92	21[b]	
14.1	5.34 ± 0.07	25[b]	
24.9	9.20 ± 0.15	43[b]	44[b]
24.9[c]	15.7 ± 0.15	38[c]	

[a] $[\text{PNAP}]_0 = 1.0 \times 10^{-5}$ M. [b] 25 °C. [c] 43 °C.

Essentially no change in ϕ occurred when the temperature was increased from 25 to 43 °C. In each experiment, PNAP exhibited good first-order kinetics to 75% conversion, as shown in Figure 3.

We performed one series of experiments in summer sunlight using quartz tubes with a constant PNAP con-

Table VI. Photolysis of PNAP/pyr in Summer Sunlight[a]

10^2[pyr], M	k_{pE}, day^{-1}	$t_{1/2}$, days measd	$t_{1/2}$, days calcd
1.60	0.18	3.8	2.7
3.38	0.39	1.8	1.4
6.09	0.71	0.97	0.90
7.84	0.88	0.78	0.70
9.70	1.07	0.64	0.55

[a] [PNAP] = 2×10^{-5} M; clear weather in July.

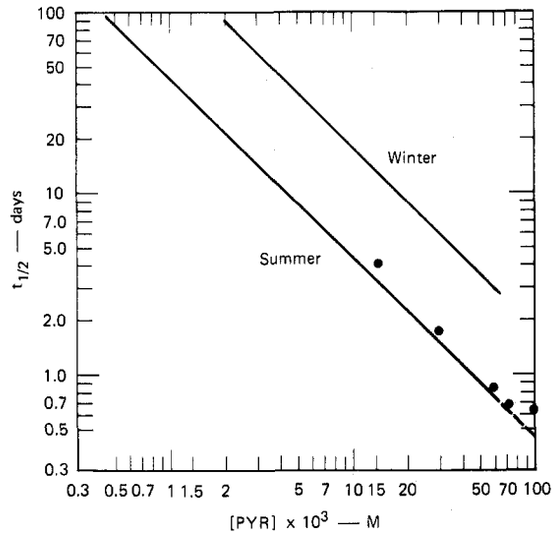

Figure 4. Calculated half-life of PNAP in sunlight as a function of [pyr] at lat 40°; (●) experimental points. Values are for tube measurements.

centration but varying pyr over a 6-fold range to measure k_{pE} and $t_{1/2(E)}$. We also calculated k_{pE} and $t_{1/2(E)}$ for photolysis of PNAP as function of [pyr] at lat 40° in summer, by using eq 1, the values of ϕ in Table V, and the values of L_λ for the interval 299–430 nm. Table VI summarizes the results. For convenience half-lives for PNAP as a function of [pyr] are plotted in Figure 4 for summer and winter.

Attempts to characterize the products from the reaction have met with only limited success. We have shown by HPLC that 1 equiv of NO_3^- ion is formed on photolysis, apparently via oxidation of first-formed NO_2^- ion. This result, if confirmed, points to a process analogous to that found for PNA with pyridine, in which a nitro group is displaced to form the pyridinium salt (eq 9). We have

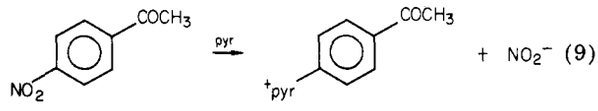

not yet succeeded in isolating this product. The excellent kinetic behavior exhibited by PNA and PNAP indicates that these products do not interfere with the photochemical processes of interest.

Evaluation of PNAP/pyr Actinometer in Sunlight. To evaluate the photolysis screening protocols using an actinometer, we selected dibenzothiophene (DBT) as a test chemical and simultaneously exposed aqueous solutions of DBT and PNAP/pyr to sunlight in quartz tubes for periods as long as 240 h (10 days elapsed time). The PNAP/pyr actinometer was adjusted to give a half-life of close to 4 days under late summer clear sky conditions; the initial [pyr] was 0.022 M. In previous studies in this laboratory (5) DBT had a quantum yield in water of 5×10^{-4} at 313 nm [$t_{1/2(E)}$ = 6 days (borosilicate)].

Table VII. Sunlight Photolysis of PNAP and DBT[a]

time, days	10^5[PNAP], M[b]	10^6[DBT], M
0	2.00	2.60
2	1.34	1.68
4	0.842	1.13
6	0.578	0.707
10	0.288	0.479
	k_{pE} = 0.19 day^{-1}	k_{pE} = 0.16 day^{-1}

[a] In quartz tubes. [b] [pyr] = 0.022 M.

Table VIII. Theoretical Sunlight Absorption Values for DBT and PNAP at lat 40°

$\Sigma L_\lambda \epsilon_\lambda$, day^{-1}	DBT	PNAP/pyr
k_p	0.17	0.19
summer	189	412
spring	87.7	201
midexperiment (May 14, 1981)	117[a]	262

[a] Absorption values are weighted averages for summer and spring.

Table VII summarizes analytical results for DBT and PNAP/pyr and gives values of k_{pE} for each chemical. In quartz, both DBT and PNAP have half-lives of about 4 days. Thus the actinometer served as a useful monitor of the changing sunlight intensity during exposure of DBT.

The quantum yield for DBT was calculated from eq 3; a regression slope of 1.107 (r = 0.997) was obtained from ln ($[PNAP]_0/[PNAP]_t$) vs. ln ($[DBT]_0/[DBT]_t$) and used in eq 3, with values of sunlight absorbance calculated from the UV spectrum of each chemical and L_λ values of Mabey et al. (1). A quantum yield of 3.8×10^{-4} for PNAP was obtained from eq 8. Relevant data are given in Table VIII.

The quantum yield for DBT in sunlight was estimated as 7.5×10^{-4}, which agrees fairly well with the value measured at 313 nm in this laboratory 3 years ago (5).

Conclusions

We believe that the PNA/pyr and PNAP/pyr actinometers will prove to be valuable tools for estimating accurate values of quantum yields for photolysis of chemicals in water. Although we have emphasized the need for and application of these actinometers for sunlight measurements, they are also useful in the laboratory where ϕ is measured at a single wavelength, usually 313 or 366 nm. In this application, the adjustable quantum yield and low sensitivity to room light also offer great advantages over conventional actinometers, which typically require handling in darkened rooms and short exposure times (6).

Work is continuing in this laboratory to evaluate these actinometers for sunlight measurements of ϕ_{cE} for several different chemicals. Results will be reported in later papers.

Acknowledgments

John Davenport and John Winterle made many helpful suggestions during the course of this work.

Literature Cited

(1) Mabey, W. R.; Mill, T.; Hendry, D. G. In "Test Protocols for Environmental Processes: Photolysis in Water"; EPA Final Report EPA 600/3-82-022, 1982; pp 49–102.
(2) *Fed. Regist.* **1979**, 16240–16292.
(3) Zepp, R. G.; Cline, D. M. *Environ. Sci. Technol.* **1977**, *11*, 359.
(4) Zepp, R. G.; Schlotzhauer, P. F. *Chemosphere* **1981**, *10*, 479.

(5) Mill, T.; Mabey, W. R.; Baraze, A.; Lan, B. *Chemosphere* **1981**, *10*, 1281.
(6) Calvert, J. G.; Pitts, J. N. "Photochemistry"; Wiley: New York, 1967.
(7) Turro, N. J. "Modern Molecular Photochemistry"; Benjamin/Cummings: Menlo Park, CA, 1978.
(8) Zepp, R. G. *Environ. Sci. Technol.* **1978**, *12*, 327.
(9) Letsinger, R. L.; Colb, A. L. *J. Am. Chem. Soc.* **1972**, *94*, 3665.
(10) Cornelisse, J.; Havinga, E. *Chem. Rev.* **1975**, *75*, 353.
(11) Letsinger, R. L.; Ramsay, O. B.; McCain, J. H. *J. Am. Chem. Soc.* **1965**, *87*, 2945.
(12) Dulin, D.; Winterle, J.; Mabey, W.; Tse, D.; Mill, T., SRI unpublished results, 1981–1982.

Received for review February 1, 1982. Accepted August 2, 1982. This work was supported by subcontract T-6416-7197-030 from Battelle Columbus Laboratories and EPA Contract 68-01-6325. Although the research described in this article has been funded wholly or in part by the U.S. Environmental Protection Agency through Contract 68-01-6325 to SRI International, it has not been subjected to the agency's required peer and policy review and therefore does not necessarily reflect the views of the Agency, and no official endorsement should be inferred.

Entrapment of Zinc and Other Trace Elements in a Rapidly Flushed Industrialized Harbor

Scott A. Sinex and George R. Helz*

Department of Chemistry, University of Maryland, College Park, Maryland 20742

■ Baltimore Harbor possesses an unusual three-layer circulation system that causes its water to be renewed at about 10% per day. Despite this rapid flushing, very fine grained argillaceous sediments accumulate in its upper reaches and appear to trap effectively trace-element contaminants such as zinc. Accumulated anthropogenic zinc in Harbor sediments is estimated to be (21–62) × 10^3 Mg, and the historic discharge of anthropogenic zinc is estimated to be about 42 × 10^3 Mg. In places, zinc has been mixed to depths greater than 3 m below the sediment–water interface. In recent decades, about 0.9 × 10^6 Mg/year of sediment in the Harbor has been displaced by dredging, and this activity has probably contributed to the plowing of contaminants into the Harbor bottom.

Introduction

Baltimore Harbor, in the Patapsco subestuary of the Chesapeake Bay system, is well-known to many estuarine scientists because of its unusual three-layer circulation (*1*, *2*). This causes water in the Harbor to be renewed at a rate of about 10% per day (*3*). It would be reasonable to expect that contaminants from the numerous industrial sources fringing the harbor would be rapidly transported into the main stem of Chesapeake Bay by the rapid flushing. However, previous studies of trace elements in the sediments from the main stem of the Bay provided little evidence for this (*4*). Therefore, we have become interested in the dynamics of contaminant transport in the Harbor. In this paper some geochemical data on Harbor sediments will be presented. Particular use will be made of zinc as an indicator of where contaminated materials are being deposited.

Sample and Locality Information

A total of 13 gravity cores and 22 surface grab samples were collected from Baltimore Harbor during May and June 1981. The plastic core liners had a diameter of 7 cm. Earlier work found this size core to have minimal compaction and foreshortening on collection (*5*). The locations are shown in Figure 1A. Samples from two deep cores near Fort McHenry in the Harbor were obtained from the Maryland State Highway Administration.

Baltimore Harbor is located on the drowned Pleistocene Valley of the Patapsco River, which is a small tributary to the Chesapeake Bay. Because the fresh water inflow of the Patapsco River is small, a circulation pattern is developed and controlled by the density or salinity distribution in the adjacent Chesapeake Bay (*1*, *2*). Fresh water inflow occurs at the surface and saline water inflow occurs near the bottom (Figure 1B). Outflow of intermediate salinity water occurs at middepth. This constitutes the major mechanism for exchange or renewal of water in the Harbor (*1*).

Carpenter (*3*) established the water renewal rate by observing the effect of acid waste discharges on alkalinity in the Harbor. This rate yields a complete turnover of Harbor water in about 10 days. Earlier estimates of 110 days by Garland (*6*) using tidal exchange were shown to be wrong. The effect of the three-layer circulation system has probably been enhanced over the last 75 years due to deepening of the channel into the Harbor (*7*).

Dredging in Baltimore Harbor began in the early 1800s and by 1836 was a federal government operation. By 1852 a complete channel from Fort McHenry to the deep water of the main Bay was completed (*8*). Gross and Cronin (*9*) estimated that 1.2 × 10^8 m^3 of materials were dredged from Baltimore Harbor between 1925 and 1975. Disposal records are limited; however, most of the disposal was overboard into sites near the operations. Records of the Baltimore Department of Public Works show that in the 1940s most disposal was done at a site outside the Harbor, slightly south of station A (Figure 1A).

With Gross and Cronin's (*9*) estimate, converted to an average annual rate of dredging (2.4 × 10^6 m^3/year), and with assumption that this dredged material contains 70% water and has a density of 1.25 Mg/m^3 (*10*), the dry weight of material dredged from Baltimore Harbor was 0.9 × 10^6 Mg/year. This number is an estimate for approximately the last 50 years and on a year-to-year basis varied considerably. This average dry weight of dredged material is comparable to the suspended sediment discharge of the Susquehanna River, which was 0.9 × 10^6 Mg/year for the period 1966–1976, excluding major floods (*11*). Not all of the Harbor dredged material was deposited in the main Bay, especially in more recent years when disposal sites within the Harbor have been used.

Gottschalk (*8*) presented evidence that high rates of siltation have occurred in the upper Harbor especially near the mouth of the Patapsco River. This area was navigable 200 years ago, but today it is a marsh. This siltation problem was caused by uncontrolled erosion occurring

 0013-936X/82/0916-0820$01.25/0